Nat1 promotes translation of specific proteins that induce differentiation of mouse embryonic stem cells

Hayami Sugiyama[a], Kazutoshi Takahashi[a,b], Takuya Yamamoto[a,c,d], Mio Iwasaki[a], Megumi Narita[a], Masahiro Nakamura[a], Tim A. Rand[b], Masato Nakagawa[a], Akira Watanabe[a,c,e], and Shinya Yamanaka[a,b,1]

[a]Department of Life Science Frontiers, Center for iPS Cell Research and Application, Kyoto University, Kyoto 606-8507, Japan; [b]Gladstone Institute of Cardiovascular Disease, San Francisco, CA 94158; [c]Institute for Integrated Cell-Material Sciences, Kyoto University, Kyoto 606-8501, Japan; [d]Japan Agency for Medical Research and Development-Core Research for Evolutional Science and Technology (AMED-CREST), Tokyo 100-0004, Japan; and [e]Japan Science and Technology Agency (JST)-CREST, Saitama 332-0012, Japan

Contributed by Shinya Yamanaka, November 22, 2016 (sent for review October 18, 2016; reviewed by Katsura Asano and Keisuke Kaji)

Novel APOBEC1 target 1 (*Nat1*) (also known as "*p97*," "*Dap5*," and "*Eif4g2*") is a ubiquitously expressed cytoplasmic protein that is homologous to the C-terminal two thirds of eukaryotic translation initiation factor 4G (*Eif4g1*). We previously showed that *Nat1*-null mouse embryonic stem cells (mES cells) are resistant to differentiation. In the current study, we found that NAT1 and eIF4G1 share many binding proteins, such as the eukaryotic translation initiation factors eIF3 and eIF4A and ribosomal proteins. However, NAT1 did not bind to eIF4E or poly(A)-binding proteins, which are critical for cap-dependent translation initiation. In contrast, compared with eIF4G1, NAT1 preferentially interacted with eIF2, fragile X mental retardation proteins (FMR), and related proteins and especially with members of the proline-rich and coiled-coil–containing protein 2 (PRRC2) family. We also found that *Nat1*-null mES cells possess a transcriptional profile similar, although not identical, to the ground state, which is established in wild-type mES cells when treated with inhibitors of the ERK and glycogen synthase kinase 3 (GSK3) signaling pathways. In *Nat1*-null mES cells, the ERK pathway is suppressed even without inhibitors. Ribosome profiling revealed that translation of mitogen-activated protein kinase kinase kinase 3 (*Map3k3*) and son of sevenless homolog 1 (*Sos1*) is suppressed in the absence of *Nat1*. Forced expression of *Map3k3* induced differentiation of *Nat1*-null mES cells. These data collectively show that *Nat1* is involved in the translation of proteins that are required for cell differentiation.

Nat1 | Eif4g1 | translation control | Map3k3 | mouse embryonic stem cells

NAT1 (novel APOBEC1 target 1), also known as "eIF4G2," "p97," and "DAP5," was identified and reported by multiple groups in 1997 (1–4). NAT1 is homologous to the C-terminal two thirds of eukaryotic translation initiation factor 4G (eIF4G) (also known as "eIF4G1"), suggesting its role in translation (5–7). In mammalian cells, translation is initiated by many eukaryotic translation initiation factors (eIFs) and other RNA-binding proteins. A key translation initiation factor is the 7-methylguanosine (m7G) cap-binding complex eIF4F, which is composed of the cap-binding subunit eIF4E, the scaffold eIF4G, and the helicase eIF4A. The small ribosomal preinitiation complex loaded with a multifactor complex including the eIF2:GTP:Met–tRNAi ternary complex and eIF3 is initially recruited to the 5′ m7G-cap of mRNA via eIF4F and then moves in the 3′ direction scanning for the initiation codon (8, 9). The eIF4A helicase unwinds secondary structures in the 5′ UTR. The largest factor eIF3 (comprised of 13 subunits) interacts with the solvent side of the small ribosomal subunit, mediating functional placement of other initiation factors. eIF4G1 forms the major contact site with the preinitiation complex. NAT1 binds to eIF4A (1, 2) and eIF3 (2) but not to eIF4E (1, 2). Therefore, it has been suggested that NAT1 is involved in noncanonical, cap-independent translation initiation of specific mRNAs. However, the precise mode of action of NAT1 and its target mRNAs is still largely unknown. To elucidate the physiological functions of NAT1, we previously knocked out its gene in mice (10). *Nat1*-null mice were lethal in uterus, before implantation, demonstrating Nat1's critical role in early development.

To study the role of *Nat1* in cell differentiation further, we generated mouse embryonic stem cells (mES cells) lacking both alleles of the *Nat1* gene. mES cells were derived from blastocysts in 1981 (11, 12) and possess two unique properties. First, ES cells have the potential to self-renew indefinitely (maintenance). Second, ES cells have the potential to differentiate into all somatic and germ cell types (pluripotency) that make up the body. We found that, even in the absence of *Nat1*, mES cells could self-renew and maintain indefinite growth properties (10). In marked contrast, when we tried to induce differentiation by removing feeder cells or by treating mES cells with retinoic acid, *Nat1*-null mES cells failed to differentiate properly. These findings demonstrated that *Nat1* is critical for the pluripotency but not for the maintenance of mES cells.

A few years after our demonstration of the differentiation-defective phenotype of *Nat1*-null mES cells, Ying et al. reported that mES cells acquire a homogeneous and completely undifferentiated status when treated with inhibitors of the *Erk* and *Gsk3b* kinase pathways (13). They designated this state the "ground state." We noticed that the morphology of *Nat1*-null mES cells was similar to that of the ground state, suggesting that *Nat1* deletion may result in changes that are similar to the ground state. In the current study, we analyzed *Nat1*-null mES cells in more detail to examine whether they are indeed in the ground state. We

Significance

We have previously shown that novel APOBEC1 target 1 (NAT1), which is homologous to the C-terminal two thirds of eukaryotic translation initiation factor 4G (eIF4G), is essential for differentiation of mouse embryonic stem cells (mES cells). In the current study, we demonstrate that *Nat1* supports the translation of mitogen-activated protein kinase kinase kinase 3 (*Map3k3*) and son of sevenless homolog 1 (*Sos1*). Deletion of *Nat1* resulted in decreased protein levels of these factors, resulting in suppression of the *Erk* and *Akt* signaling pathway. Forced expression of *Map3k3* induced differentiation in *Nat1*-null mES cells. Thus *Nat1* is involved in the translation of proteins that are required for the differentiation of mES cells.

Author contributions: H.S. and S.Y. designed research; H.S., K.T., T.Y., M.I., M. Narita, M. Nakamura, and T.A.R. performed research; S.Y. provided supervision; H.S., K.T., T.Y., M.I., M. Nakamura, M. Nakagawa, and A.W. analyzed data; and H.S. and S.Y. wrote the paper.

Reviewers: K.A., Kansas State University; and K.K., University of Edinburgh.

Conflict of interest statement: S.Y. is a scientific advisor of iPS Academia Japan without salary.

Freely available online through the PNAS open access option.

Data deposition: The accession numbers for mRNA microarray data for comparison of LIF or LIF + 2i-cultured WT and *Nat1*-null mouse ES cells, the effects of *Map3k3* expression in *Nat1*-null mouse ES cells, and ribosome profiling data reported in this paper have been deposited in the Gene Expression Omnibus database (accession nos. GSE89007, GSE89600, and GSE89011, respectively).

[1]To whom correspondence should be addressed. Email: yamanaka@cira.kyoto-u.ac.jp.

This article contains supporting information online at www.pnas.org/lookup/suppl/doi:10.1073/pnas.1617234114/-/DCSupplemental.

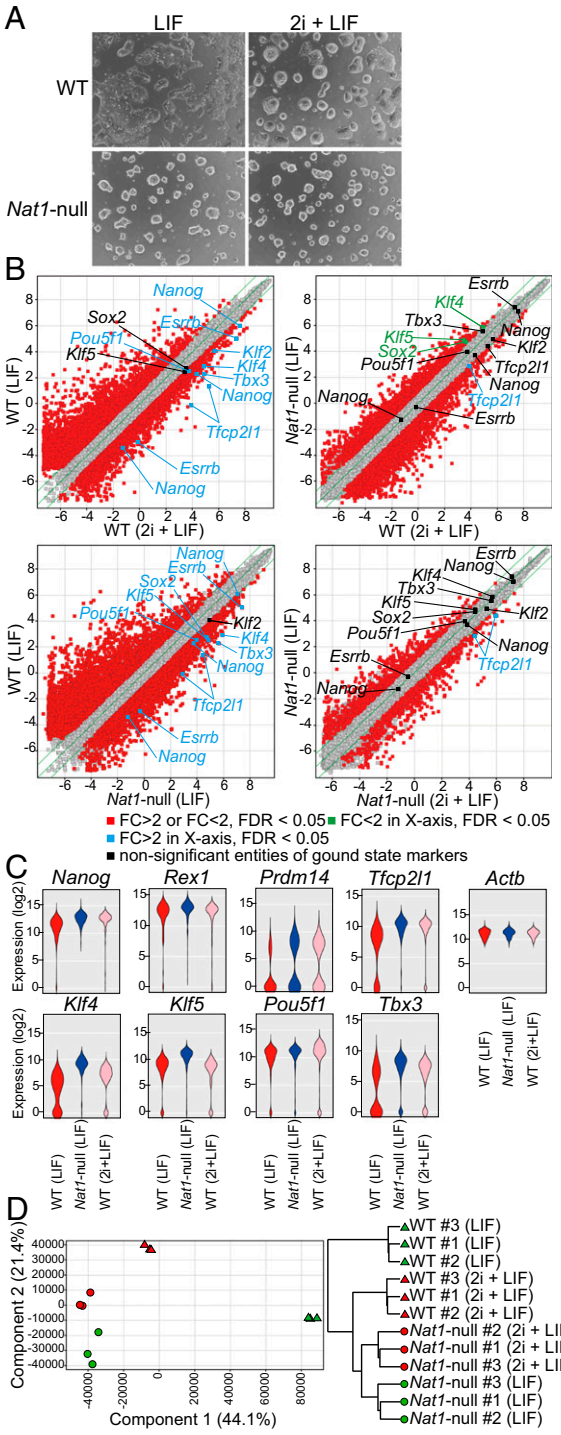

Fig. 1. *Nat1*-null mES cells show a status similar but not identical to the ground state. (*A*) The morphology of WT mES cells and *Nat1*-null mES cells cultured in LIF or 2i+LIF 3 days after reseeding on gelatin-coated dishes. (*B*) Scatter plots of transcript expression in *Nat1*-null and WT mES cells. The expression values are shown on a log2 scale. Red dots indicate probes with significantly different expressions ($n = 3$, twofold FDR <0.05) between the samples on the *x* axis and *y* axis; blue dots indicate core transcription factors enriched in the ground state that are expressed more than twofold on the *x* axis than on the *y* axis; green dots indicate factors that are expressed more than twofold on the *y* axis; black dots indicate factors with no significant difference between on the *x* and *y* axes. (*C*) Violin plots of cycle threshold value (log2 scale) of mRNA expression in single cells. Samples were collected 3 days after reseeding on gelatin-coated dishes. (*D*) PCA and hierarchical clustering analyses of WT and *Nat1*-null mES cells.

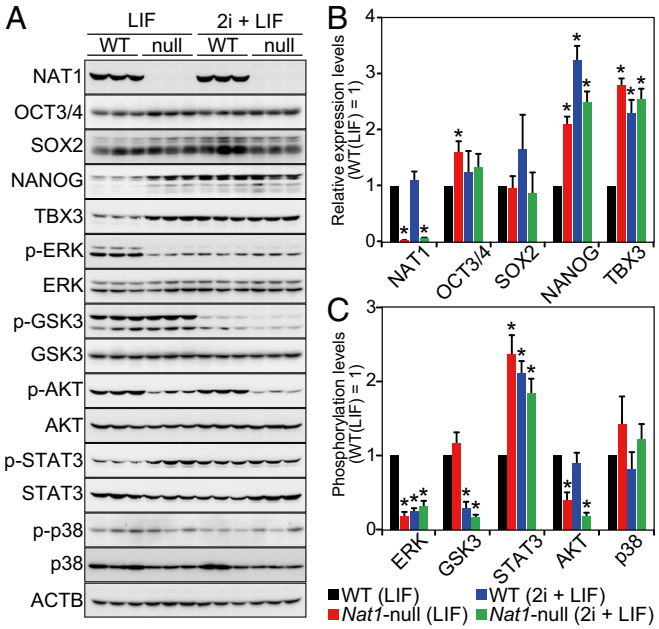

Fig. 2. Intracellular signaling was altered in *Nat1*-null mES cells. (*A*) Protein expression of NAT1, OCT3/4, SOX2, NANOG, TBX3, ERK, GSK3, AKT, STAT3, p38, and ACTB, as well as phosphorylated (p-) ERK, p-GSK3, p-AKT, p-STAT3, and p-p38 in WT and *Nat1*-null ES cells by Western blotting analyses. (*B*) Quantification of protein expression levels normalized with ACTB. Values in LIF-treated WT mES cells were set to 1. $*P < 0.05$, $**P < 0.01$, *t* test; $n = 3$. Error bars indicate SD. (*C*) Quantification of phosphorylation levels, normalized with ACTB. Values in LIF-treated WT mES cells were set to 1. $*P < 0.05$, *t* test; $n = 3$. Error bars indicate SD.

also performed immunoprecipitation (IP), MS, and ribosome-profiling analyses to understand better the molecular interactions and the translational impact of *Nat1*.

Results

***Nat1*-Null mES cells Show a Status Similar but Not Identical to the Ground State.** *Nat1*-null mES cells maintained in the standard ES cell-culture condition with leukemia inhibitory factor (LIF) showed a round, dome-like morphology resembling that of WT mES cells cultured with the two kinase inhibitors and LIF (2i+LIF) (Fig. 1*A*). To compare gene expression in *Nat1*-null and WT mES cells, we performed microarray analyses (Fig. 1*B*). In WT mES cells, the mRNA expressions of several transcription factors, including *Nanog*, *Esrrb*, *Klf2*, *Klf4*, *Tbx3*, *Pou5f1* (also known as "*Oct3/4*"), and *Tfcp2l1* were increased significantly when treated with 2i+LIF (shown in red in Fig. 1*B*, *Upper Left*). Even without the two kinase inhibitors, *Nat1*-null mES cells showed higher expression levels of transcription factors that are more highly expressed in the ground state than in the primed state (Fig. 1*B*, *Lower Left*), comparable to the levels seen in WT mES cells treated with 2i+LIF (Fig. 1*B*, *Upper Right*). The 2i treatment did not induce a further increase of these genes in *Nat1*-null mES cells (Fig. 1*B*, *Lower Right*). Single-cell quantitative RT-PCR (qRT-PCR) also demonstrated that *Nat1*-null mES cells were similar to the ground state in terms of higher and more uniform expression of several key transcription factors (Fig. 1*C*). However, the global gene expression was not identical in *Nat1*-null mES cells and ground-state mES cells: Many genes were differentially expressed (Fig. 1*B*, *Upper Right*). Principal component analysis (PCA) and hierarchical clustering analysis confirmed that the gene expression profile of *Nat1*-null mES cells was similar but not identical to that of ground-state mES cells. (Fig. 1*D*).

Intracellular Signaling in *Nat1*-Null ES Cells. To address the effects of *Nat1* deletion on intracellular signaling, we performed Western

CELL BIOLOGY

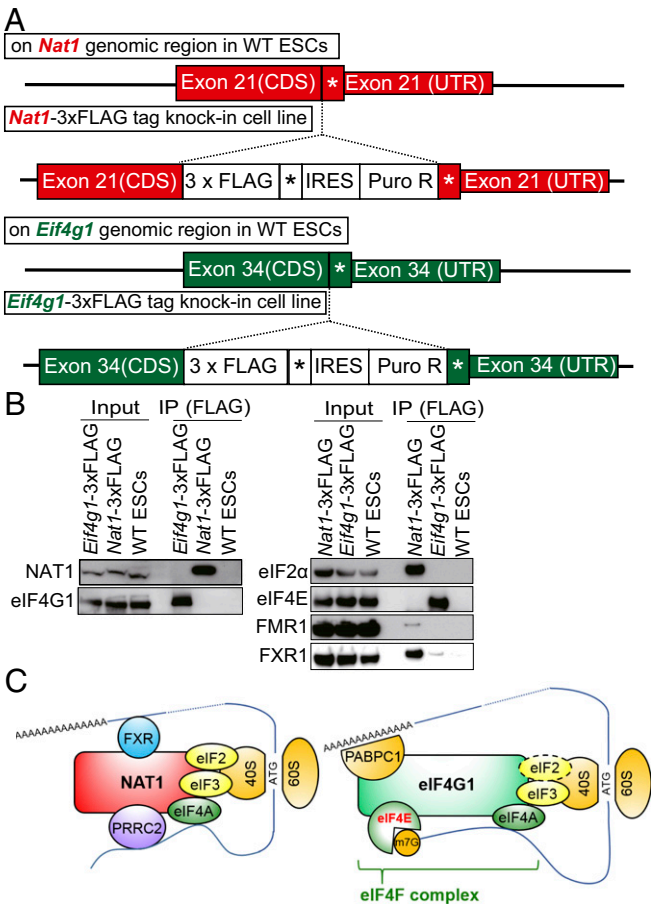

Fig. 3. NAT1 and eIF4G1 form unique translational complexes. (*A*) The locus of the 3×FLAG-tag knocked into the *Nat1* or *Eif4g1* sites using the CRISPR/Cas9 (nickase; D10A) system. (*B*) Western blot analyses of *Nat1*-3×FLAG-IP and *Eif4g1*-3×FLAG-IP samples. (*C*) Models of cap-dependent translation with eIF4G1 and cap-independent translation with NAT1. The dashed circle indicates a very small amount of eIF2 bound to eIF4G1.

blot analyses (Fig. 2). We confirmed that the expression of OCT3/4, NANOG, and TBX3 increased to a similar degree in *Nat1*-null mES cells and ground-state mES cells (Fig. 2 *A* and *B*). Of note, we found that the phosphorylation level of ERK1/2 decreased markedly, whereas that of STAT3 was increased in *Nat1*-null mES cells, similar to levels in the ground state (Fig. 2 *A* and *C*). In contrast, phosphorylation of other signaling molecules, including GSK3β and p38, did not change. We also observed decreased phosphorylation of AKT in *Nat1*-null mES cells. These findings demonstrated that specific signaling pathways are altered as a result of *Nat1* deletion.

NAT1 and EIF4G1 Form Unique Translational Complexes. To identify NAT1-binding proteins, we prepared mES cells in which the 3×FLAG tag was knocked into the 3′ end of the *Nat1* or *Eif4g1* coding region by using the CRISPR/Cas9 system (Fig. 3*A*) (14). After IP with an anti-FLAG antibody, we identified coimmunoprecipitated proteins by MS analysis with the iTRAQ system, which measures relative peptide abundances precisely. We found that NAT1 and eIF4G1 shared many binding proteins, such as eIF4A1 and 2, ribosomal proteins, and all 13 eIF3 subunits except eIF3j, which is a loosely associated subunit (Table 1 and Table S1). NAT1 did not bind to eIF4E, as previously reported (1, 2). In addition, eIF4G1, but not NAT1, strongly bound to the poly(A)-binding protein PABPC1 and to the cleavage and polyadenylation specificity factor CPSF3. Importantly, NAT1 preferentially bound to eIF2 (15), FMR1, FXR1 (16), and members of proline-rich coiled-coil–containing protein 2 family, including PRRC2A, PRRC2B, and PRRC2C (Table 1). Western blot confirmed preferential binding of eIF2α, FMR1, and FXR1 to NAT1 (Fig. 3*B*). Thus, NAT1 and eIF4G1 form overlapping but unique protein complexes (Fig. 3*C*).

Suppressed Translation of MAP3K3 and SOS1 in *Nat1*-Null mES cells. To identify mRNAs translationally regulated by NAT1, we performed ribosome profiling (17), which quantifies the ribosome-protected mRNA fragment (RPF) to determine translationally active regions on mRNA (Fig. 4*B* and Table S2). We compared WT, *Nat1* heterozygous ($Nat1^{+/-}$), and *Nat1*-null ($Nat1^{-/-}$) mES cells. $Nat1^{+/-}$ mES cells showed a normal phenotype in development and had the same characteristics as WT mES cells (10). First, we visualized mapped fragments for the *Nat1* gene locus (Fig. 4*A*). Total mRNA signals showed that exons 1 and 2 were not expressed in *Nat1*-null mES cells, consistent with our targeting strategy with which we eliminated the second exon containing the translational initiation codon. Interestingly, the remaining exons were still expressed, but the signals of the 3′ half decreased compared with WT and $Nat1^{+/-}$ mES cells. This decrease may be attributable to nonsense-mediated RNA decay (18). In marked contrast, RPF signals in *Nat1*-null mES cells were not detected throughout the coding-sequence regions, reflecting a depletion of *Nat1* translation resulting from the absence of the start codon. Next, we compared the normalized counts of total fragments and RPFs mapped to each gene using the Xtail pipeline (19), which has been developed to identify differentially translated genes. We identified 18 genes (14 decreased and four increased) whose translation differed by more than twofold between in WT and *Nat1*-null mES cells and between in $Nat1^{+/-}$ and *Nat1*-null mES cells (Fig. 4*B*). Of note, translationally suppressed genes included *Map3k3* and *Sos1*, which have

Table 1. Highlights of NAT1- and eIF4G1-interacting proteins

	Relative ratio of median intensity, $n = 4$		
Protein	Nat1/control	Eif4g1/ control	Nat1/Eif4g1
AP2A1	60.0	19.5	2.4
AP2M1	7.8	2.7	2.2
CPSF2	1.7	7.1	0.3
CPSF3	2.5	65.6	0.1
CPSF4	4.4	9.0	0.5
eIF2α	84.1	6.7	8.5
eIF2β	93.7	4.8	12.6
eIF2γ	88.3	5.6	9.9
eIF3a	72.0	24.6	2.8
eIF3b	75.2	25.6	2.7
eIF3c	64.0	22.2	2.9
eIF3d	73.3	24.8	3.1
eIF3e	71.4	23.8	2.8
eIF3f	76.3	23.8	3.1
eIF3g	68.6	21.7	2.7
eIF3h	67.7	22.2	3.0
eIF3i	66.5	24.9	2.8
eIF3k	74.3	25.7	2.9
eIF3l	77.1	24.2	3.0
eIF3m	77.5	29.7	3.1
eIF4A1	31.0	68.1	0.4
eIF4A2	19.9	15.3	1.2
eIF4A3	1.0	2.1	0.5
eIF4E	1.0	48.5	0.0
FMR1	56.5	19.8	2.3
FXR1	60.0	14.0	3.6
FXR2	16.3	6.6	2.6
PABPC1	2.8	73.2	0.1
PRRC2A	74.8	10.0	4.9
PRRC2B	94.4	4.4	18.4
PRRC2C	78.8	12.6	4.6
TRIM71	43.4	43.7	1.0

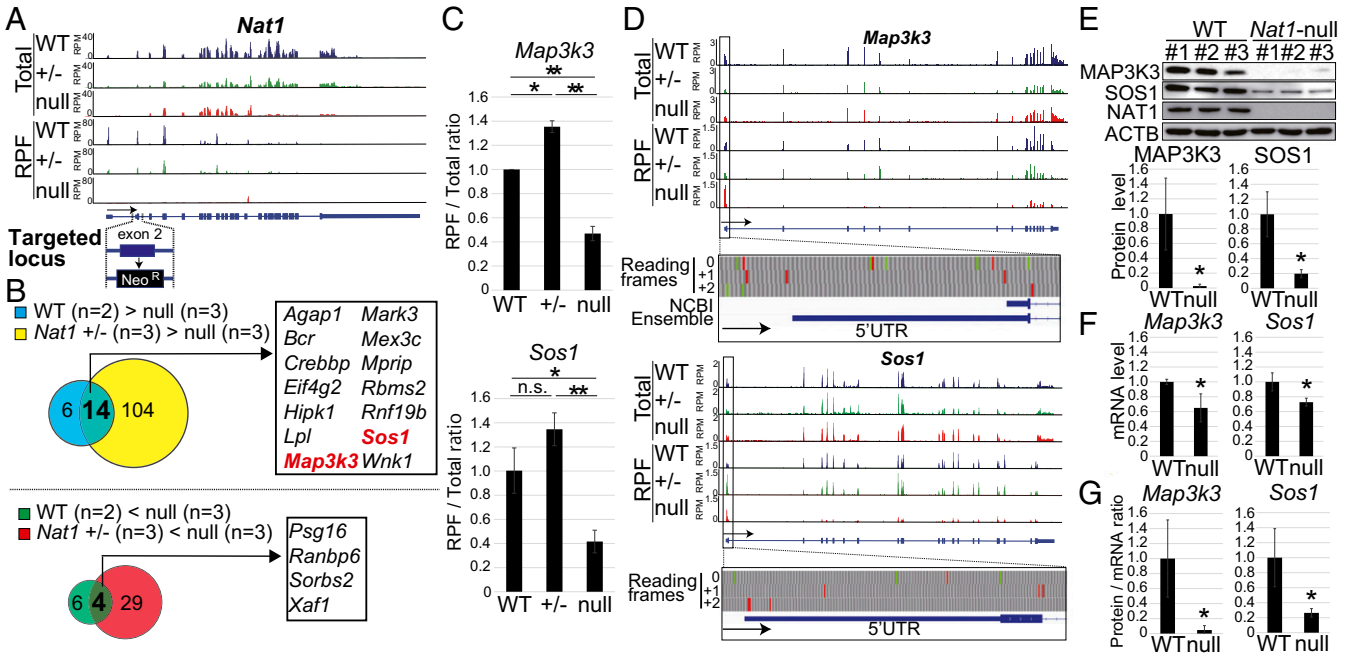

Fig. 4. Ribosome profiling demonstrates decreased translation of MAP3K3 and SOS1. (*A*) Distribution of expressed mRNA fragments (total) and RPFs on the *Nat1* transcript and the *Nat1*-targeted locus. (*B*) Venn diagram of candidates whose translations were promoted (*Upper*) or suppressed (*Lower*) by *Nat1*. Shown are the number of mRNAs whose RPF/total ratios differed by more than twofold in WT mES cells and in *Nat1*-null mES cells (left circles, $P < 0.01$) and in *Nat1*$^{+/-}$ and in *Nat1*-null mES cells (right circles $P < 0.01$). Lists of mRNAs overlapping in the two comparisons are shown in the inserted tables. (*C*) RPF/total expressed mRNA fragment ratios in WT mES cells, *Nat1*$^{+/-}$ mES cells, and *Nat1*-null mES cells cultured in LIF. Values in WT mES cells cultured with LIF were set to 1. Averages and ±SD are shown. *$P < 0.05$, **$P < 0.01$; n.s., no significant, *t* test. (*D*) Distribution of total expressed mRNA fragments, RPFs, and upper ORFs on *Map3k3* and *Sos1* transcripts. Gray rows indicate three different reading frames. Green squares indicate predicted initiation codons (methionine). Red indicates stop codons. The National Center for Biotechnology Information (NCBI) and Ensemble gene IDs for *Map3k3* are NM_001947 and ENMUST00000002044, respectively. The NCBI gene ID for *Sos1* is NM_009231. (*E*) Protein levels of MAP3K3 and SOS1 in WT and *Nat1*-null mES cells cultured with LIF determined by Western blot. Quantification of the protein expression levels was adjusted with ACTB. Values in LIF-treated WT mES cells were set to 1. *$P < 0.05$, *t* test; $n = 3$. Error bars indicate SD. (*F*) mRNA expression levels of *Map3k3* and *Sos1* in LIF-treated WT and *Nat1*-null mES cells by qRT-PCR. The expression levels were adjusted with *Actb* and normalized to those in WT mES cells. (*$P < 0.05$, *t* test; $n = 3$). Error bars indicate SD. (*G*) Protein/mRNA ratios of *Map3k3* and *Sos1* calculated from qRT-PCR (*F*) and Western blot (*E*). *$P < 0.05$, *t* test; $n = 3$. Error bars indicate SD.

been reported to be upstream of Erk1/2 in the MAPK pathway (20, 21). The ratios of RPF/total fragments of *Map3k3* and *Sos1* were significantly lower in *Nat1*-null mES cells than in WT or *Nat1*$^{+/-}$ mES cells (Fig. 4*C*). Interestingly, both *Map3k3* and *Sos1* mRNAs possess alternative ORFs in the 5′ UTR (Fig. 4*D*). Western blot analyses confirmed that protein levels of MAP3K3 and SOS1 decreased markedly in *Nat1*-null mES cells (Fig. 4*E*). In contrast, their mRNA levels decreased only slightly (Fig. 4*F*). Thus, the protein/mRNA ratios of *Map3k3* and *Sos1* in *Nat1*-null mES cells were approximately 5% and 25% of those in WT mES cells (Fig. 4*G*).

Forced Expression of *Map3k3* Induced Differentiation in *Nat1*-Null mES cells. To determine whether *Map3k3* and *Sos1* can rescue the differentiation-defective phenotypes of *Nat1*-null mES cells, we introduced tetracycline (tet)-inducible *Map3k3*- or EGFP-, *Sos1*-, or DsRed-expressing cassettes into *Nat1*-null mES cells. In the absence of doxycycline, these cells maintained the round, dome-shaped morphology typical of *Nat1*-null mES cells (Fig. 5 *A* and *B*). In marked contrast, *Map3k3*-expressing *Nat1*-null mES cells showed a morphological change indicative of differentiation after the addition of doxycycline at a final concentration of 0.02 μg/mL. In these cells, phosphorylation of ERK reverted to the WT level (Fig. 5*C*). The mRNA expression of several pluripotency-related transcription factors, including *Nanog*, *Pou5f1*, *Sox2*, *Esrrb*, and *Klf4*, decreased significantly in these cells (Fig. 5*D*). In addition, the mRNA expression levels of differentiation markers including *Gata3*, *Gata6*, *Sox17*, and *Foxa2* increased (Fig. 5*E*). The transcript levels of *Brachyury* (also known as "*T*") and *Fgf5* did not change. *Sos1*-expressing *Nat1*-null mES cells did not change morphologically after the addition of doxycycline. These findings indicated that the suppressed translation of *Map3k3* partially contributes to the impaired differentiation of *Nat1*-null mES cells.

Discussion

In this study, we showed that *Nat1* deletion results in a status similar but not identical to the ground-like state, which normally is induced by kinase inhibitors. IP followed by MS analyses demonstrated that NAT1 interactions are distinct from those of eIF4G1. In addition, ribosome profiling showed that NAT1 is involved in the translation of proteins that play critical roles in cell differentiation.

MEK inhibition is critically important in the induction of the ground state (13). It alone can induce the ground status, although in an unstable manner. We found that translation of MAP3K3 and SOS1 was suppressed in the absence of *Nat1*. The two proteins are involved in the ERK signaling pathway at different levels. *Map3k3* is one of many MAP kinase kinase kinases and activates ERK and other MAP kinases (20). *Sos1* is one of the *Ras*-specific guanine nucleotide exchange factors that convert *Ras* from inactive *Ras*·GDP to active *Ras*·GTP (22). Inactivation of these genes in mice resulted in defects in MAPK activity and in utero development (23, 24). We also found that forced expression of *Map3k3* induced differentiation in *Nat1*-null mES cells. Therefore, it is reasonable to suggest that the translational suppression of these two proteins contributes, at least in part, to the observed attenuation of the ERK signal and the ground-state–like property in *Nat1*-null mES cells.

Both *Map3k3* and *Sos1* mRNAs have short upstream ORFs (uORFs). Because uORFs are considered to be translational repressors (25, 26), we hypothesize that these elements repress the translation of these mRNAs after cell differentiation. In WT mES cells, we propose that *Nat1* alleviates this translational repression

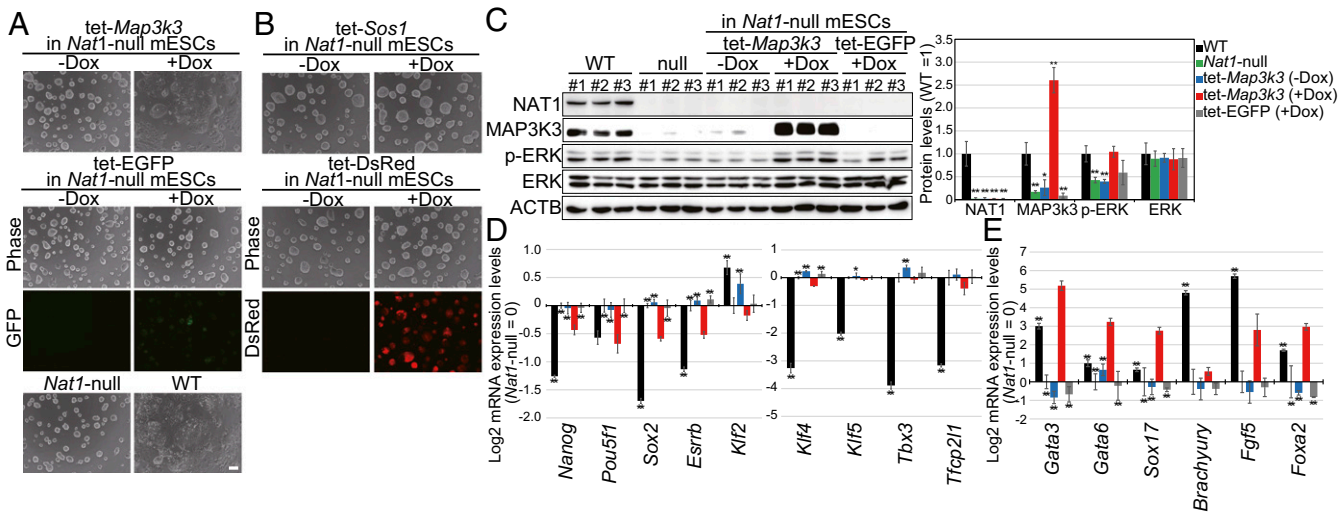

Fig. 5. Forced expression of *Map3k3* induces differentiation in *Nat1*-null mES cells. (*A*) Morphology of *Nat1*-null mES cells expressing tet-inducible *Map3k3* or EGFP. Cells were cultured in standard mES cell medium containing LIF with or without doxycycline (Dox; final concentration 0.02 μg/mL) on gelatin-coated dishes. (Scale bar, 100 μm.) (*B*) Morphology of *Nat1*-null mES cells expressing tet-inducible *Sos1* or DsRed. Cells were cultured in standard mES cell medium containing LIF with or without doxycycline (final concentration 0.125 μg/mL). (Scale bar, 100 μm.) (*C*) Protein expression of NAT1, p-ERK, ERK, and ACTB in *Map3k3*-expressing *Nat1*-null mES cells by Western blotting analysis. Quantification of protein expression levels was normalized with ACTB. Values in WT mES cells were set to 1. $*P < 0.05$, $**P < 0.01$, *t* test; $n = 3$. Error bars indicate SD. (*D* and *E*) Log2 mRNA expression levels of pluripotency markers (*D*) and differentiation markers (*E*) in *Map3k3*-expressing *Nat1*-null mES cells by microarray. Log2 expression values in *Nat1*-null mES cells were set to 0 ($n = 3$). Error bars indicate SD. Significant differences from the corresponding *Map3k3*-expressing *Nat1*-null mES cells: $*P < 0.05$; $**P < 0.01$, Dunnett's test.

through direct mRNA recruitment without involving eIF4E (see the model in Fig. 3*C*). Further mechanistic studies will be required to determine whether NAT1 mediates cap-independent translation of these mRNAs.

One important question is how NAT1 associates with mRNA to support cap-independent translation. Our MS analyses showed that NAT1 was coimmunoprecipitated with many eIFs and RNA-binding proteins. Some were preferentially bound to NAT1 rather than to eIF4G1. These include FMR1, its homolog FXR proteins, and PRRC2 proteins. Recently, NAT1, together with FXR1 was shown to mediate noncanonical translation initiation of specific mRNA in quiescent and immature oocytes (16). PRRC2 proteins have been listed in three previous articles (27–29) that systemically identified RNA-binding proteins. Otherwise, little is known about the functions of PRRC2 proteins. Further studies are required to understand the roles of these and other RNA-binding proteins in the translation of *Map3k3* and *Sos1*.

In conclusion, we have demonstrated that *Nat1* promotes the translation of differentiation-promoting proteins in mES cells. Considering the abundant and ubiquitous expression of *Nat1*, we speculate that its role is not confined to *Map3k3* and *Sos1*. Our data also showed that the translation of certain mRNAs may be suppressed by NAT1 (Fig. 4*B*). In *Nat1*-null mES cells, the mRNA expression levels of numerous genes are altered from those of WT counterparts. This alteration makes it difficult to estimate translation efficiency from ribosome profiling. Further studies, such as conditional deletion of *Nat1* and identification of *Nat1*-binding proteins for translational regulation, are required for a better understanding of *Nat1*'s cap-independent translational mechanism.

Materials and Methods

Cell Lines and Culture Conditions. The RF8 WT mES cell line was derived from 129/TerSv mice, and *Nat1*$^{+/-}$ and *Nat1*-null mES cells were generated from the RF8 mES cell line in our previous study (10). mES cells were maintained in DMEM (Nacalai Tesque, 08459-64) containing 15% (vol/vol) FBS (Gibco, 10437-028), 50 units·50 μg^{-1}·mL^{-1} penicillin/streptomycin (Gibco, 15149-122), 0.11 mM 2-Mercaptoethanol (Gibco, 21985-023), 2 mM L-glutamine (Gibco, 25030-081), 0.1 mM MEM nonessential amino acids (Gibco, 1140-050), and LIF, as previously described (30), on dishes coated with 0.1% gelatin (Sigma, G1890-500G). We called this mES cell standard medium "LIF" and called the medium with two added inhibitors [MEK inhibitor (1 mM PD0325901; Stemgent 04-006) and Gsk3 inhibitor (3 mM CHIR99021; Stemgent 04-004)] "2i+LIF." The primers and antibodies used for the qRT-PCR and Western blot experiments using these ES cells are listed in Tables S3 and S4, respectively.

Generation of *Nat1*- or *Eif4g1*-3×FLAG Knock-In mES cells. The 3×FLAG knock-in target regions for *Nat1* and *Eif4g1* were amplified by PCR and subcloned with the 3×FLAG sequence before the stop codon into the pENTR/D-TOPO vector as 3×FLAG knock-in targeting vectors using the Cold Fusion Cloning Kit (System Biosciences, MC010A-1). Guide RNA (gRNA) vectors for *Eif4g1* contained the gRNA target sequences gRNA *Eif4g1* R1, ACAACCGTGATCTACCATCC, and gRNA *Eif4g1* F1, GTCTTTTTGGGAGGGATCTC; gRNA vectors for *Nat1* contained the gRNA target sequences gRNA *Eif4g2* R1, GGAAAGGGCCACCGGACCCT, and gRNA *Eif4g2* F1, GTGGCCCTTTCGGGCTGCCG. To generate *Nat1*-3×FLAG knock-in ES cells and *Eif4g1*-3×FLAG knock-in ES cells using the CRISPR/Cas9 system (14), the targeting vectors, gRNA vector sets, and nickase (D10A) (31) expression vectors were cotransfected into WT mES cells (RF8) using Lipofectamine 2000 Reagent (Invitrogen, 11668-019) according to the manufacturer's instructions. Twenty-four hours after transfection, cells were selected with puromycin (final concentration 1 μg/mL) for three passages and picked to isolate each clone.

Generation of Tet-Inducible *Map3k3*-, *Sos1*-Expressing *Nat1*-Null mES cells. The ORFs of *Map3k3* and *Sos1* were amplified by PCR and reacted with the pENTR/D-TOPO vector. Each *Map3k3* ORF or EGFP ORF was cloned into PB-TAC-ERP2 (32), and each *Sos1* ORF or DsRed ORF was cloned into PB-TAG-ERP2 using a Gateway LR reaction (Invitrogen) according to the manufacturer's instructions. To generate tet-inducible *Map3k3*-, *Sos1*-expressing *Nat1*-null mES cells, the PB-TAC-ERP2/*Map3k3*, PB-TAC-ERP2/EGFP, PB-TAG-ERP2/*Sos1*, or PB-TAG-ERP2/DsRed vector was transfected into *Nat1*-null mES cells using Xfect mESC Transfection Reagent (Clontech, 631320) according to the manufacturer's instructions. Twenty-four hours after transfection, cells were selected with puromycin (final concentration 1 μg/mL) for three passages. To express the genes, doxycycline (final concentration 0.02 μg/mL for *Map3k3* and EGFP or 0.125 μg/mL for *Sos1* and DsRed) was supplemented with standard mES cell medium.

IP-MS Sample Preparation and Data Collection. Protein reduction/alkylation, Lys-C/trypsin digestion (enzyme ratio: 1/100), and desalting of the samples were performed as described previously (33). After labeling with isobaric tags for relative and absolute quantification (iTRAQ, AB Sciex), each peptide sample was suspended and mixed in the loading buffer [0.5% trifluoroacetic acid and 4% (vol/vol) acetonitrile] for subsequent nanoLC-MS/MS analysis. NanoLC-MS/MS was performed using a TripleTOF 5600 System (AB Sciex) equipped with an HTC-PAL autosampler (CTC Analytics). Loaded samples were separated on a self-pulled analytical column (150-mm length, 100-μm i.d.) using a Dionex

UltiMate 3000 RSLCnano System. The mobile phases consisted of (A) 0.5% acetic acid with 5% (vol/vol) DMSO and (B) 0.5% acetic acid in 80% (vol/vol) acetonitrile with 5% (vol/vol) DMSO (34). A three-step gradient condition of 5–10% (vol/vol) B in 5 min, 10–40% (vol/vol) B in 60 min, 40–100% (vol/vol) B in 5 min was used with a flow rate of 500 μL/min, and a spray voltage of 2,300 V was applied. The MS scan range was 300−1500 *m/z* every 0.25 s. Triplicate analyses were conducted for each sample, and blank runs were inserted between different samples.

IP-MS Data Analyses. The raw data files were analyzed by ProteinPilot v5.0 (AB Sciex). Peak lists, which were generated from the ProteinPilot.group file, were analyzed by Mascot v2.5 (Matrix Science). Both database search engines were used against UniProt/Swiss-Prot release 2015_06 (27 May 2015) with the previously described parameters (33), with the exception of a precursor mass tolerance of 20 ppm and a fragment ion mass tolerance of 0.1 Da. For protein identification, peptides were grouped into protein groups based on previously established rules (35). Then at least two confidently identified peptides per protein were used for the identification. A minimum peptide length of six amino acids and single peptides with higher confidence ($P < 0.01$) were also used for the identification. False discovery rates (FDRs) were estimated by searching against a decoy sequence database (<1%). For protein quantification, the intensity of the iTRAQ label spectra was normalized by i-Tracker Perl script (36), and the median value of the iTRAQ label ratio was calculated for each protein.

Single-Cell Expression qRT-PCR Analysis. Single cells were captured on a C1 Single-Cell Auto Prep System with an integrated fluidic circuit (IFC) chip for cells 10- to 17-μm long (Fluidigm, 100-5480), and the cDNAs were preamplified using the SMART-Seq v4 Ultra Low Input RNA Kit for Sequencing (Clontech, 634894) and pooled primers according to the manufacturer's instructions. qPCR of the amplified cDNAs was performed using SsoFast EvaGreen Supermix with Low ROX (Bio-Rad Laboratories, 1725210B04), nested primers (Table S5), and the Biomark HD system (Fluidigm) with a 96.96 Dynamic Array IFC chip (Fluidigm, BMK-M10-96.96). Cycle threshold values were calculated using Fluidigm's Real-Time PCR Analysis software. Log2-transformated expression values were calculated using the SINGuLar Analysis Toolset (Fluidigm).

Ribosome Profiling. Ribosome profiling was performed using WT mES cells ($n = 2$, one clone), *Nat1*$^{+/-}$ mES cells ($n = 3$, three clones), and *Nat1*-null mES cells ($n = 3$, three clones). RPF and total RNA libraries were prepared using the TruSeq Ribo Profile Mammalian Kit (Illumina) according to the manufacturer's instructions. The obtained libraries were sequenced on a NextSeq 500 system (Illumina). Bases with low-quality scores and the adapters in all sequenced reads were trimmed with cutadapt-1.9.1 (37). The trimmed reads were mapped to mouse rRNA and tRNA sequences with Bowtie2 version 2.2.8 (38), and the reads aligned to rRNA or tRNA were excluded from further analysis. The remaining reads were mapped to the mouse genome (mm10) using TopHat-2.1.0 (39) with GENCODE annotation (GRCm38.p4, release M10) (40). The number of reads mapped to each gene was counted by HTSeq-0.6.1 software (41) and normalized with the DESeq2 R/Bioconductor package (v. 1.10.1) (42). Differentially translated genes were identified with the Xtail pipeline (v 1.1.5) (19).

ACKNOWLEDGMENTS. We thank Dr. Knut Woltjen for kindly providing PB-tet–inducible vectors; Dr. Akitsu Hotta for providing D10A and gRNA vectors; Dr. Toshiki Taya for guidance in gene-expression analyses; Toshiko Sato, Mio Kabata, and Satoko Sakurai for technical assistance in ribosome profiling analysis; Midori Sakiyama, Marina Kishida, and Chihiro Okada for technical assistance in single-cell qRT-PCR analysis; Rie Kato, Sayaka Takeshima, Yoko Miyake, and Hitomi Imagawa for administrative support; Dr. Peter Karagiannis for critical reading of the manuscript; and the members of the Center for iPS Cell Research and Application for valuable discussions. This work was supported by a grant from the Core Center for iPS Cell Research, Research Center Network for Realization of Regenerative Medicine from the Japan Agency for Medical Research and Development and by the iPS Cell Research Fund.

1. Yamanaka S, Poksay KS, Arnold KS, Innerarity TL (1997) A novel translational repressor mRNA is edited extensively in livers containing tumors caused by the transgene expression of the apoB mRNA-editing enzyme. *Genes Dev* 11(3):321–333.
2. Imataka H, Olsen HS, Sonenberg N (1997) A new translational regulator with homology to eukaryotic translation initiation factor 4G. *EMBO J* 16(4):817–825.
3. Shaughnessy JD, Jr, Jenkins NA, Copeland NG (1997) cDNA cloning, expression analysis, and chromosomal localization of a gene with high homology to wheat eIF-(iso)4F and mammalian eIF-4G. *Genomics* 39(2):192–197.
4. Levy-Strumpf N, Deiss LP, Berissi H, Kimchi A (1997) DAP-5, a novel homolog of eukaryotic translation initiation factor 4G isolated as a putative modulator of gamma interferon-induced programmed cell death. *Mol Cell Biol* 17(3):1615–1625.
5. Hentze MW (1997) eIF4G: A multipurpose ribosome adapter? *Science* 275(5299):500–501.
6. Morley SJ, Curtis PS, Pain VM (1997) eIF4G: Translation's mystery factor begins to yield its secrets. *RNA* 3(10):1085–1104.
7. Gingras AC, Raught B, Sonenberg N (1999) eIF4 initiation factors: Effectors of mRNA recruitment to ribosomes and regulators of translation. *Annu Rev Biochem* 68:913–963.
8. Asano K, Clayton J, Shalev A, Hinnebusch AG (2000) A multifactor complex of eukaryotic initiation factors, eIF1, eIF2, eIF3, eIF5, and initiator tRNA(Met) is an important translation initiation intermediate in vivo. *Genes Dev* 14(19):2534–2546.
9. Asano K, Sachs MS (2007) Translation factor control of ribosome conformation during start codon selection. *Genes Dev* 21(11):1280–1287.
10. Yamanaka S, et al. (2000) Essential role of NAT1/p97/DAP5 in embryonic differentiation and the retinoic acid pathway. *EMBO J* 19(20):5533–5541.
11. Evans MJ, Kaufman MH (1981) Establishment in culture of pluripotential cells from mouse embryos. *Nature* 292(5819):154–156.
12. Martin GR (1981) Isolation of a pluripotent cell line from early mouse embryos cultured in medium conditioned by teratocarcinoma stem cells. *Proc Natl Acad Sci USA* 78(12):7634–7638.
13. Ying QL, et al. (2008) The ground state of embryonic stem cell self-renewal. *Nature* 453(7194):519–523.
14. Ran FA, et al. (2013) Double nicking by RNA-guided CRISPR Cas9 for enhanced genome editing specificity. *Cell* 154(6):1380–1389.
15. Lee SH, McCormick F (2006) p97/DAP5 is a ribosome-associated factor that facilitates protein synthesis and cell proliferation by modulating the synthesis of cell cycle proteins. *EMBO J* 25(17):4008–4019.
16. Bukhari SI, et al. (2016) A specialized mechanism of translation mediated by FXR1a-associated microRNP in cellular quiescence. *Mol Cell* 61(5):760–773.
17. Ingolia NT, Ghaemmaghami S, Newman JR, Weissman JS (2009) Genome-wide analysis in vivo of translation with nucleotide resolution using ribosome profiling. *Science* 324(5924):218–223.
18. Baker KE, Parker R (2004) Nonsense-mediated mRNA decay: Terminating erroneous gene expression. *Curr Opin Cell Biol* 16(3):293–299.
19. Xiao Z, Zou Q, Liu Y, Yang X (2016) Genome-wide assessment of differential translations with ribosome profiling data. *Nat Commun* 7:11194.
20. Craig EA, Stevens MV, Vaillancourt RR, Camenisch TD (2008) MAP3Ks as central regulators of cell fate during development. *Dev Dyn* 237(11):3102–3114.
21. Findlay GM, et al. (2013) Interaction domains of Sos1/Grb2 are finely tuned for cooperative control of embryonic stem cell fate. *Cell* 152(5):1008–1020.
22. Margarit SM, et al. (2003) Structural evidence for feedback activation by Ras.GTP of the Ras-specific nucleotide exchange factor SOS. *Cell* 112(5):685–695.
23. Yang J, et al. (2000) Mekk3 is essential for early embryonic cardiovascular development. *Nat Genet* 24(3):309–313.
24. Wang DZ, et al. (1997) Mutation in Sos1 dominantly enhances a weak allele of the EGFR, demonstrating a requirement for Sos1 in EGFR signaling and development. *Genes Dev* 11(3):309–320.
25. Barbosa C, Peixeiro I, Romão L (2013) Gene expression regulation by upstream open reading frames and human disease. *PLoS Genet* 9(8):e1003529.
26. Johnstone TG, Bazzini AA, Giraldez AJ (2016) Upstream ORFs are prevalent translational repressors in vertebrates. *EMBO J* 35(7):706–723.
27. Castello A, et al. (2012) Insights into RNA biology from an atlas of mammalian mRNA-binding proteins. *Cell* 149(6):1393–1406.
28. Baltz AG, et al. (2012) The mRNA-bound proteome and its global occupancy profile on protein-coding transcripts. *Mol Cell* 46(5):674–690.
29. Castello A, et al. (2016) Comprehensive identification of RNA-binding domains in human cells. *Mol Cell* 63(4):696–710.
30. Takahashi K, Yamanaka S (2006) Induction of pluripotent stem cells from mouse embryonic and adult fibroblast cultures by defined factors. *Cell* 126(4):663–676.
31. Li HL, et al. (2015) Precise correction of the dystrophin gene in Duchenne muscular dystrophy patient induced pluripotent stem cells by TALEN and CRISPR-Cas9. *Stem Cell Rep* 4(1):143–154.
32. Kim SI, et al. (2016) Inducible transgene expression in human iPS cells using versatile all-in-one piggyBac transposons. *Methods Mol Biol* 1357:111–131.
33. Yamana R, et al. (2013) Rapid and deep profiling of human induced pluripotent stem cell proteome by one-shot NanoLC-MS/MS analysis with meter-scale monolithic silica columns. *J Proteome Res* 12(1):214–221.
34. Hahne H, et al. (2013) DMSO enhances electrospray response, boosting sensitivity of proteomic experiments. *Nat Methods* 10(10):989–991.
35. Nesvizhskii AI, Aebersold R (2005) Interpretation of shotgun proteomic data: The protein inference problem. *Mol Cell Proteomics* 4(10):1419–1440.
36. Shadforth IP, Dunkley TP, Lilley KS, Bessant C (2005) i-Tracker: For quantitative proteomics using iTRAQ. *BMC Genomics* 6:145.
37. Martin M (2011) Cutadapt removes adapter sequences from high-throughput sequencing reads. *Bioinformatics in Action* 17(1):10–12.
38. Langmead B, Salzberg SL (2012) Fast gapped-read alignment with Bowtie 2. *Nat Methods* 9(4):357–359.
39. Kim D, et al. (2013) TopHat2: Accurate alignment of transcriptomes in the presence of insertions, deletions and gene fusions. *Genome Biol* 14(4):R36.
40. Harrow J, et al. (2006) GENCODE: Producing a reference annotation for ENCODE. *Genome Biol* 7(Suppl 1):S4.1–S4.9.
41. Anders S, Pyl PT, Huber W (2015) HTSeq–a Python framework to work with high-throughput sequencing data. *Bioinformatics* 31(2):166–169.
42. Love MI, Huber W, Anders S (2014) Moderated estimation of fold change and dispersion for RNA-seq data with DESeq2. *Genome Biol* 15(12):550.